

A modified SPH approach for fluids with large density differences

Frank Ott and Erik Schnetter

*Institut für Astronomie und Astrophysik, Auf der Morgenstelle, Universität Tübingen,
D-72076 Tübingen, Germany*

Abstract

We introduce a modified SPH approach that is based on discretising the particle density instead of the mass density. This approach makes it possible to use SPH particles with very different masses to simulate multi-phase flows with large differences in mass density between the phases. We test our formulation with a simple advection problem, with sound waves encountering a density discontinuity, and with shock tubes containing a contact discontinuity between air and Diesel oil. For all examined problems where particles have different masses, the new formulation yields better results than standard SPH. This is also the case for problems in which different spatial resolutions are needed while the mass density does not change.

Key words: SPH, Smoothed Particle Hydrodynamics, multi-phase flow, fluid interfaces

PACS: 02.60.Cb, 02.70.Ns

1 Motivation

SPH is a Lagrangian particle method for solving the equations of hydrodynamics that was invented by Lucy [1] and Gingold and Monaghan [2]. Instead of discretising space with a grid, the matter is discretised into so-called particles which move with the fluid and do not exchange mass. This method is especially suited for compressible flows with irregular boundaries. SPH has been used for many astrophysical problems with great success, and has also been applied to other fields of physics, such as e.g. the simulation of liquids [3] and solids [4,5].

Email address: schnetter@uni-tuebingen.de (Erik Schnetter).

Due to its Lagrangian nature, simulating several non-mixing fluids is a straightforward extension to SPH. Each particle gets initially marked with the phase it belongs to, and these marks do not change with time.

We are interested in simulating compressible flows with large density differences in contact discontinuities, e.g. due to an interface between a jet of liquid near the speed of sound in a surrounding gas. Unfortunately, standard SPH as e.g. presented in [6,7] breaks down in this case, as explained in this text. Previous approaches to handle large density differences in SPH (e.g. [8]) rely on ad-hoc countermeasures.

For subsonic flows, [9] presents a mesh-free numerical method for gas-liquid phase interfaces which is based on the MPS method [10]. It is restricted to incompressible flows, whereas we are interested in compressible flows. We are also interested in similar spatial resolutions in both phases of the flow. This requirement is different from e.g. astrophysical collapse simulations, where one usually wants a higher resolution in the denser regions.

Another point of interest for us is having differing spatial resolutions, i.e. particles with different masses, in regions where the mass density does not change. This has been used on several occasions (e.g. in [11]). However, this can lead to rather large errors with standard SPH.

We will in the following present a modification of SPH that interprets certain numerical quantities in a different manner [12], leading to a stable, robust, and accurate evolution even in these cases.

2 Describing multi-phase flows

One commonly used way of introducing the SPH discretisation (see also [7]) starts out by considering an arbitrary field $f(\mathbf{x})$. This field is first *smoothed* by folding it with a kernel $W(\mathbf{x})$, which leads to the smoothed field $\langle f(\mathbf{x}) \rangle$

$$\langle f(\mathbf{x}) \rangle := \int d^3x' f(\mathbf{x}') W(\mathbf{x} - \mathbf{x}') \quad (1)$$

where the kernel $W(\mathbf{x})$ must be normalised according to $\int d^3x W(\mathbf{x}) = 1$. One usually chooses kernels that have approximately the shape of a Gaussian, and that have compact support for reasons of efficiency. The size of the domain of support is called the *smoothing length* and is usually denoted with the letter h .

In the next step, the smoothing integral is discretised at N particle positions

\mathbf{x}_i , which can in principle be chosen freely, but should of course be “reasonably” distributed. This leads to the *SPH approximation* $\tilde{f}(\mathbf{x})$

$$\tilde{f}(\mathbf{x}) := \sum_{j=1}^N V_j f_j W(\mathbf{x} - \mathbf{x}_j) \quad (2)$$

of the field. The volumes V_j are the discrete counterparts of the volume element d^3x' in the integral above, and have to be chosen so as to be consistent with the spatial distribution of the particles. It is customary to assign a certain mass m_i to each particle, and then replace the volumes through

$$V_i = \frac{m_i}{\rho_i} \quad (3)$$

where ρ_i is the discretised mass density assigned to the particle. This is motivated by the fact that the particles do not exchange mass, which leads to the time evolution equation

$$\frac{d}{dt} m_i = 0 \quad (4)$$

making m_i a natural choice for one of the primary variables. In order to make SPH Lagrangian, the particles have to move with the flow, leading to

$$\frac{d}{dt} \mathbf{x}_i = \mathbf{v}_i \quad (5)$$

as the time evolution equation for the particle positions \mathbf{x}_i . Here \mathbf{v}_i is the discretised fluid velocity field.

Assuming that the desired spatial resolution is about the same in all fluid phases, one would choose similar particle spacings there, leading to similar particle volumes V_i . If the mass densities in the different fluids are about the same, no further problems arise, and SPH as usual can be used to describe them. However, if the difference in mass density is large (say, about one order of magnitude or more), then the particle masses will differ by the same factor, leading to problems at the phase interfaces. These problems are mostly caused by inaccuracies in the mass density. These inaccuracies are substantial for largely different particle masses. Below we describe how they come about, and how they can be avoided.

2.1 Standard SPH

There exist in principle two different methods for obtaining the discretised mass density ρ_i in the “standard” SPH formalism. Both start out by considering the approximate mass density $\tilde{\rho}$ at the particle position \mathbf{x}_i . This quantity is obtained from eqn. (2) by choosing $f(\mathbf{x}) = \rho(\mathbf{x}_i)$ and applying eqn. (3), leading to

$$\tilde{\rho}(\mathbf{x}_i) = \sum_j m_j W_{ij} \quad (6)$$

where the abbreviation $W_{ij} := W(\mathbf{x}_i - \mathbf{x}_j)$ has been introduced.

The first and conceptually simpler method to obtain ρ_i from this is by setting $\rho_i := \tilde{\rho}(\mathbf{x}_i)$, leading to

$$\rho_i = \sum_j m_j W_{ij} \quad . \quad (7)$$

This method is often used for astrophysical problems when there are free boundaries, i.e. when the matter distribution extends into vacuum. However, it is not suited for a phase interface with a large density discontinuity. The smoothing inherent in eqn. (7) will smooth out the density jump over a region of the size of the smoothing length h in either direction of the discontinuity. Particles in this region will then “see” a density that is much less or much larger from the real density in their phase. When this density is used to calculate the pressure through the two phases’ equations of state, the pressure will be very wrong (as shown in figure 1 for two ideal gases), and it is basically impossible to set up a stable interface in equilibrium. This problem becomes even more severe when one of the fluids has a stiff equation of state, as is the case e.g. in liquids or solids, because then density inaccuracies will lead to even larger errors in the pressure.

The second method for obtaining the mass density ρ_i is by integrating ρ_i in time via the time derivative of eqn. (7), leading to

$$\frac{d}{dt} \rho_i = \sum_j m_j (\mathbf{v}_i - \mathbf{v}_j) \cdot \nabla W_{ij} \quad (8)$$

where eqn. (5) has been used, and the abbreviation $\nabla W_{ij} := (\nabla W)(\mathbf{x}_i - \mathbf{x}_j)$ has been introduced. This method has the advantage that the initial data for ρ_i can be chosen freely, so that density discontinuities can be modelled. This can be used to simulate surfaces of liquids and solids.

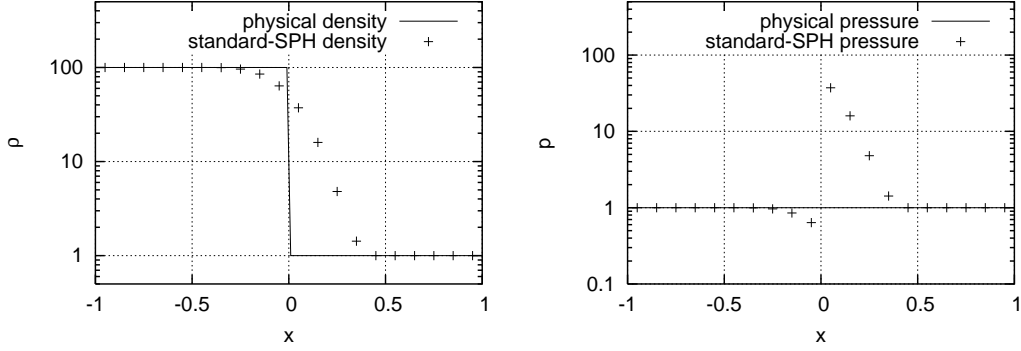


Figure 1. Physical density and pressure and the corresponding standard SPH quantities at a phase interface with equal pressure and a density ratio of 100 : 1. Near the interface, the approximation errors reach a factor of about 2 in the dense region and about 50 in the thin region. Essentially the same picture results when there is no change in mass density, but when instead the particle mass and spacing are changed by a factor of 100 to achieve a higher spatial resolution (not shown). (These approximation errors do not exist when a different SPH formulation is used; see section 2.2 below).

The problem with this method is similar to the problem encountered when calculating the density directly from the particle distribution by eqn. (7). The particles on each side of a phase interface “see”, via the term m_j in eqn. (8), very different particle masses on the other side of the interface. The values of $d/dt \rho_i$ then contain large inaccuracies, leading to instabilities at phase interfaces.

2.2 Modified SPH

However, eqn. (7) is not cast in stone. An ansatz equivalent to but different from the one leading to this equation is not to smooth the mass density ρ_i , but rather the particle density $n_i = 1/V_i$ [12]. This is easily motivated by the fact that the mass density can be discontinuous over a phase interface, while the particle density is not, according to our assumption of similar spatial resolutions on both sides. Smoothing the particle density $n_i := \tilde{n}(\mathbf{x}_i)$ via eqn. (2) leads to

$$n_i = \sum_j W_{ij} \quad (9)$$

and by taking its time derivative, the equation

$$\frac{d}{dt} n_i = \sum_j (\mathbf{v}_i - \mathbf{v}_j) \cdot \nabla W_{ij} \quad (10)$$

is obtained after using eqn. (5). As it is customary in SPH to use ρ_i instead of n_i , we apply eqns. (3) and (4) and arrive at

$$\frac{d}{dt} \rho_i = m_i \sum_j (\mathbf{v}_i - \mathbf{v}_j) \cdot \nabla W_{ij} \quad . \quad (11)$$

This new formulation of the equation of continuity is the key element of our SPH approach. It should be noted that this equation is identical to eqn. (8) when all particle masses m_i are the same, which is the case for many single-phase SPH simulations.

For the simulations presented in this text, we discretise the Euler and the internal energy equations in established ways:

$$\frac{d}{dt} \mathbf{v}_i = -\frac{1}{\rho_i} \sum_j \frac{m_j}{\rho_j} (p_j + p_i) \nabla W_{ij} \quad (12)$$

$$\frac{d}{dt} e_i = \frac{1}{2} \frac{1}{\rho_i} \sum_j \frac{m_j}{\rho_j} (p_j + p_i) (\mathbf{v}_i - \mathbf{v}_j) \cdot \nabla W_{ij} \quad (13)$$

where e_i is the specific internal energy. The symmetrisations $(p_j + p_i)$ are e.g. explained in [7].

3 Tests

In the following we test the new SPH formulation and compare it to analytic solutions as well as simulations performed using standard SPH as described in [7]. That is, the only difference between these two formulations is that we use eqn. (11) instead of eqn. (8). This also means that other parts of an SPH code such as time integration or artificial viscosity are not affected. As test cases, we use an advection problem, a sound wave encountering a discontinuous change in the sound speed, and a shock tube with a Diesel–air interface.

3.1 Advection equation

We compare the standard and the new SPH formulation by simulating a one-dimensional advection equation. That is, we solve the equation of continuity for the density ρ while prescribing the velocity field v . The velocity

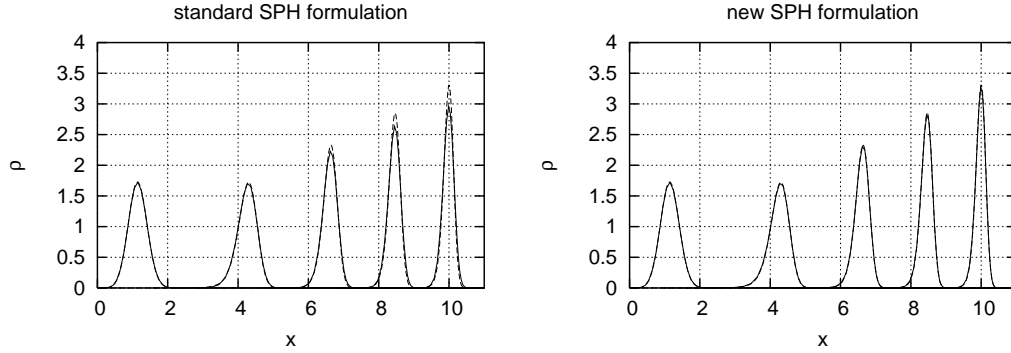


Figure 2. Comparison of simulations with the standard SPH and the new SPH formulation at five different times. The dotted lines show the analytic solution, the solid lines show the particle values. Standard SPH is less accurate at the narrower peaks, which correspond to later times.

profile (which is constant in time) and the initial density profile are given by

$$v(x) = \frac{x}{1 + qx^2} \quad (14)$$

$$\rho_0(x) = A x^2 \exp \left\{ - \left(\frac{x - x_0}{W} \right)^2 \right\} \quad (15)$$

with $A = 1.5$, $x_0 = 1$, $W = 0.4$, and $q = 0.2$. We initially place the particles with equidistant spacings with a density of $n = 10$ particles per unit length and use a smoothing length of $h = 0.25$. The particle masses are chosen according to the initial density profile at the initial particle positions, i.e. they differ. Advection problems are particularly well suited test problems for Lagrangian methods, so we expect a high accuracy from this low resolution.

The results of simulating this equation with both the standard and the new SPH formulation are presented in figure 2, which shows the density ρ at five different times. Both formulations track the analytic solution very nicely in spite of the coarse resolution. However, at later times, the standard SPH formulation underestimates the density near the peaks, while the new formulation stays much closer to the analytic solution.

3.2 Sound wave

The sound wave test case consists of two regions containing the same ideal gas, but with different densities and in pressure equilibrium. The density

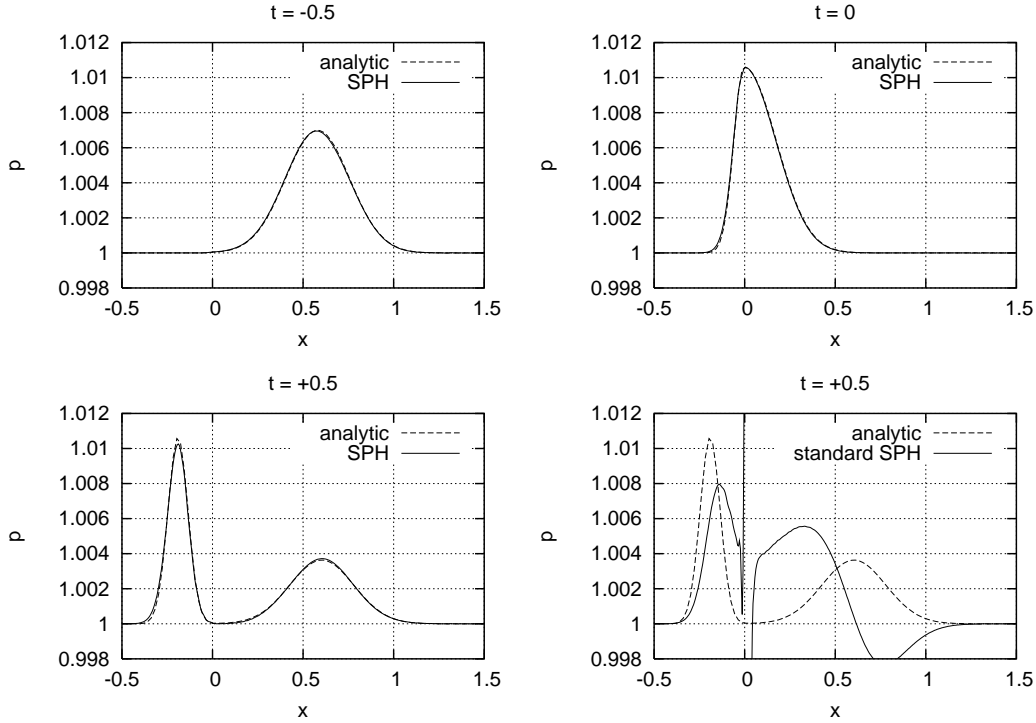


Figure 3. A sound wave crossing an interface between two ideal gases with a density ratio of 10 : 1. The interface is at $x = 0$. Shown is the pressure at the times $t = -0.5$, $t = 0$, and $t = +0.5$, where dotted lines mark the analytic solution. The graph in the lower right hand corner shows the result at $t = +0.5$ of a simulation with standard SPH for comparison.

discontinuity is located at $x = 0$ with a density ratio of 10 : 1. These conditions also lead to different temperatures, and to sound speeds with a ratio of $1 : \sqrt{10}$. Figure 3 shows an initially Gaussian-shaped sound wave at different times.

At $t = -0.5$ the initial wave travels to the left. At $t = 0$ the wave has reached the interface where it is partially transmitted and partially reflected. At $t = +0.5$ the wave consists of two packets, travelling in different directions with different speeds. The simulation was performed with $n = 200$ particles per unit length and a smoothing length of $h = 0.1$. The analytic solution is shown as dotted line underneath the simulation result. The SPH simulation with the new equation of continuity (11) tracks the analytic solution quite well. On the other hand, standard SPH using eqn. (8) performs rather poorly in this case, as can be seen in the graph in the lower right hand corner: the transmission and reflection coefficients are wrong, and the pressure develops spikes at the interface. We assume that the reason for this is just the one demonstrated in figure 1.

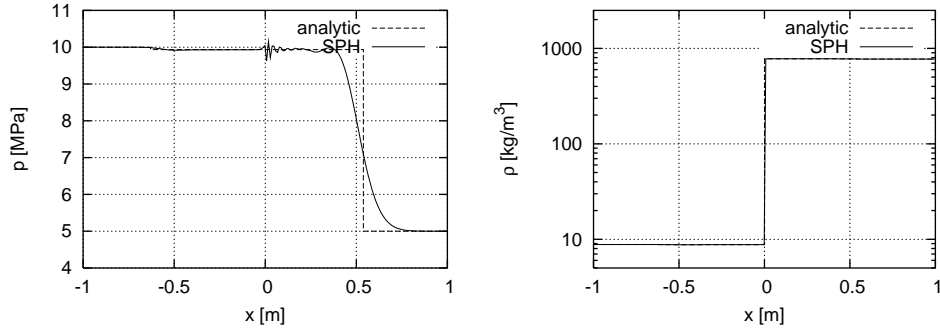


Figure 4. A shock wave emanating from an interface with air to the left and Diesel to the right. Shown are pressure and density at $t = 5 \times 10^{-4}$ s, where dotted lines mark the analytic solution. The discontinuity is initially at $x = 0$. The shock front is spread out over 8 smoothing lengths by artificial viscosity. The pressure difference across the rarefaction wave is rather small. The shock and rarefaction waves are not visible in the density graph because of the large scale differences. The contact discontinuity is stable and well preserved in spite of the coarse resolution; the pressure oscillations do not grow with time.

Table 1

Initial data for the shock tube test case

Quantity	air	Diesel oil
ρ [kg/m ³]	8.81	772.546
p [MPa]	10	5
T [K]	3931.5	393.15

3.3 Shock tube

A further test case for our formulation is a shock tube containing a Diesel–air interface, shown in figure 4. The initial discontinuity is at $x = 0$, with air to the left and (liquid) Diesel oil to the right. The initial pressure ratio is 2 : 1, the density ratio about 1 : 80. Here we have artificially decreased the air density and increased the air temperature by a factor of 10 to create a more difficult test case. Table 1 lists the exact initial data for this test case. The shock wave in the Diesel oil travels to the right, the rarefaction wave in the air to the left. Because the Diesel oil is nearly incompressible, the final pressure is close to the initial pressure in the air phase. The equation of state for the Diesel oil was kindly provided to us by the Robert Bosch GmbH.

The simulation was performed with $n = 100$ particles per metre and a smoothing length of $h = 5 \times 10^{-2}$ m. We use the artificial viscosity presented in [7] with a viscosity coefficient of $\alpha = 0.5$, because some artificial viscosity is necessary to produce entropy in the shock front. This spreads out the shock front over about 8 smoothing lengths, which is acceptable for our purposes.

Table 2

Comparison of the analytic solution and the simulation result for the shock relations in the Diesel phase. v_s is the shock front speed, v_D the post-shock Diesel speed. The sound speed in the pre-shock Diesel phase is 1059.6 m/s.

Quantity	analytic	SPH
v_s [m/s]	1077	1056 ± 20
v_D [m/s]	5.93	5.94 ± 0.02
$\Delta\rho_D$ [kg/m ³]	4.27	4.28 ± 0.02
Δp_D [MPa]	4.93	4.94 ± 0.02
ΔT_D [K]	0.860	0.855 ± 0.005

The initial pressure discontinuity remains visible as spikes at the contact discontinuity. These spikes are caused by the numerical initial data, which have a discontinuity and hence contain high frequency modes that are not resolved in the simulation. According to eqn. (1), the initial data should be smoothed before the SPH formalism is applied. We skip this step because we want to show that these high frequency modes do not harm the simulations. They remain present, but are not amplified. The formulation is stable. Table 2 compares several important quantities of the simulation result to the analytic solution, showing very good agreement in the shock relations.

We did not manage to perform this simulation with standard SPH. As illustrated in figure 1, the error in the density near the contact discontinuity leads to an error in the pressure. The pressure error can be orders of magnitude larger than the pressure itself for fluids which have a stiff equation of state. This problem does not exist in the new formulation.

4 Conclusion

We describe a modification to the standard SPH formalism that smoothes the particle density instead of the mass density. As tested by simulating an advection equation, sound waves, and shock waves, the new formulation either yields more accurate results than standard SPH, or the equivalent simulation with standard SPH is not stable. We conclude that this modified SPH formulation is an effective method for simulating multi-phase flows, and conjecture that this modification is beneficial for all simulations where particles have different masses.

The authors would like to thank Prof. Hanns Ruder for encouraging this work. We would also like to thank the Robert Bosch GmbH for providing an equation of state for Diesel oil. Financial support was provided by the

Robert Bosch GmbH and the Ministerium für Wissenschaft und Forschung
in Baden-Württemberg.

References

- [1] L. B. Lucy, A numerical approach to the testing of the fission hypothesis, *Astron. J.* 82 (12) (1977) 1013–1024.
- [2] R. A. Gingold, J. J. Monaghan, Smoothed particle hydrodynamics: theory and application to non-spherical stars, *Mon. Not. R. Astron. Soc.* 181 (1977) 375–389.
- [3] J. J. Monaghan, Simulating free surface flows with SPH, *J. Comp. Phys.* 110 (1994) 399–406.
- [4] W. Benz, W. L. Slattery, A. G. W. Cameron, The origin of the moon and the single-impact hypothesis. I, *Icarus* 66 (1986) 515–535.
- [5] W. Benz, W. L. Slattery, A. G. W. Cameron, The origin of the moon and the single-impact hypothesis. II, *Icarus* 71 (1987) 30–45.
- [6] J. J. Monaghan, R. A. Gongold, Shock simulations by the particle method SPH, *J. Comp. Phys.* 52 (1983) 374–389.
- [7] J. J. Monaghan, Smoothed particle hydrodynamics, *Annu. Rev. Astron. Astrophys.* 30 (1992) 543–574.
- [8] B. W. Ritchie, P. A. Thomas, Multiphase smoothed-particle hydrodynamics, *Mon. Not. R. Astron. Soc.* 323 (2001) 743–756.
- [9] H. Y. Yoon, S. Koshizuka, Y. Oka, A mesh-free numerical method for direct simulation of gas-liquid phase interface, *Nucl. Sci. Eng.* 133 (1999) 192–200.
- [10] S. Koshizuka, H. Tamako, Y. Oka, A particle method for incompressible viscous flow with fluid fragmentation, *Comp. Fluid Dynamics J.* 4 (1) (1995) 29–46.
- [11] S. Kunze, R. Speith, F. V. Hessman, Substantial stream-disc overflow found in three-dimensional SPH simulations of cataclysmic variables, *Mon. Not. R. Astron. Soc.* 322 (2001) 499–514.
- [12] F. Ott, Weiterentwicklung und Untersuchung von Smoothed Particle Hydrodynamics im Hinblick auf den Zerfall von Dieselfreistrahlen in Luft, Ph.D. thesis, Universität Tübingen (1999).